Available online at www.sciencedirect.com

ScienceDirect

Journal of Otology 12 (2017) 185–191

www.journals.elsevier.com/journal-of-otology/

Temporal bone anatomy characteristics in superior semicircular canal dehiscence

Marrigje A. de Jong [a], David J. Carpenter [b], David M. Kaylie [b], Erin G. Piker [c], Dennis O. Frank-Ito [b,d,e,*]

[a] Department of Otorhinolaryngology/Head and Neck Surgery, Hadassah Hebrew University Hospital, Jerusalem, Israel
[b] Division of Head and Neck Surgery & Communication Sciences, Duke University Medical Center, Durham, NC, USA
[c] Department of Communication Sciences and Disorders, James Madison University, Harrisonburg, VA, USA
[d] Computational Biology & Bioinformatics, Duke University, Durham, NC, USA
[e] Department of Mechanical Engineering and Materials Science, Duke University, Durham, NC, USA

Received 18 June 2017; revised 31 July 2017; accepted 4 August 2017

Abstract

Introduction: Superior semicircular canal dehiscence (SCD) remains difficult to diagnose despite advances in high-resolution computed tomography (HRCT) imaging. We hypothesize possible associations between gross temporal bone anatomy and sub-millimeter pathology of the semicircular canals, which may supplement imaging and clinical suspicion. This pilot study investigates differences in gross temporal bone anatomic parameters between temporal bones with and without SCD.

Methods: Records were reviewed for 18 patients referred to an otology clinic complaining of dizziness with normal caloric stimulation results indicative of non-vestibular findings. Eleven patients had normal temporal bone anatomy while seven had SCD. Three-dimensional reconstruction of every patient's temporal bone anatomy was created from patient-specific computational tomography images. Surface area (SA), volume (V), and SA to V ratios (SA:V) were computed across temporal bone anatomical parameters.

Results: SCD temporal bones have significantly smaller V, and larger temporal bone SA. Mean (±SD) V was 21,484 ± 3,921 mm^3 in temporal bones without SCD and 16,343 ± 34,471 mm^3 for those with SCD. Their respective SA were 13,733 ± 1,603 mm^2 and 18,073 ± 3,002 mm^2. Temporal bone airspaces and lateral semicircular canals did not demonstrate significant differences where SCD was and was not present. Plots of MV_{warm} response against computed SCD temporal bone anatomic parameters (SA, V and SA:V) showed moderate to strong correlations: temporal bone SA:V ($r = 0.64$), temporal bone airspace V ($r = 0.60$), temporal bone airspace SA ($r = 0.55$), LSCC SA ($r = 0.51$), and LSCC-to-TM Distance ($r = 0.65$).

Conclusions: This analysis demonstrated that SCD is associated with decreased temporal bone volume and density. The defect in SCD does not appear to influence caloric responses.

Keywords: Temporal bone; Anatomy; Superior canal dehiscence; Superior semicircular canal dehiscence

1. Introduction

Superior semicircular canal dehiscence (SCD) involves discontinuity of the bone overlying the superior semicircular canal (SSCC), creating a third window in the inner ear. Normal pressure gradients for the endolymphatic flow are disturbed and patients typically present with auditory and

* Corresponding author. Division of Head and Neck Surgery & Communication Sciences, Department of Surgery, Box 3805, Duke University Medical Center, Durham, NC 27710, USA. Fax: +1 919 613 6524.
E-mail address: dennis.frank@duke.edu (D.O. Frank-Ito).

Peer review under responsibility of PLA General Hospital Department of Otolaryngology Head and Neck Surgery.

http://dx.doi.org/10.1016/j.joto.2017.08.003

vestibular symptoms such as hyperacousis, autophony, oscillopsia and vertigo induced by loud sound or pressure (Ho et al., 2017). High-resolution computed tomography (HRCT) is the preferred imaging modality for confirming SCD. However, false positive radiologic findings and asymptomatic radiographically apparent dehiscence limit the diagnostic utility of HRCT. These scans do not permit differentiation of bone thinner than 0.1 mm from true dehiscence. In normal subjects, bone overlying the SSCC has an average thickness of 0.67 mm and standard deviation of 0.38 mm, and the proportion of normal individuals with an overlying SC bone thickness <0.1 mm is greater than the incidence of SCD in the general population (0.05%) (Carey et al., 2000). Accordingly, the positive predictive value of HRCT for SCD is only 57% (Cloutier et al., 2008).

Given the diagnostic limitations of HCRT, SCD is confirmed in the clinical setting by additional physiologic tests including audiometry and calorimetry. Audiometric findings associated with SCD include air-bone gaps and negative bone conduction thresholds at lower frequencies (Ho et al., 2017) Caloric testing is commonly performed in patients with SCD due to associated complaints of vertigo. However, the utility of caloric testing as a diagnostic tool for SCD has been questioned because the SSCC is not reached by caloric stimulation (Ichijo, 2012). The relationship of temporal bone anatomy to caloric output has been described in previous reports of healthy subjects, and may represent an additional means of identifying subjects with SCD based on their temporal bone anatomy (Patki et al., 2016).

Pursuing additional SCD diagnostic strategies is warranted. We hypothesize that SCD may demonstrate unique anatomic characteristics at the level of the gross temporal bones that may assist clinicians in cases where HRCT findings are indeterminate at the SSCC. This hypothesis is based on previous characterizations of SCD anatomy that demonstrated a propensity for uniform SSCC bone thickness bilaterally in patients with and without SCD (Carey et al., 2000; Hirvonen et al., 2003; Gracia-Tello et al., 2013). However, the clinical applicability of these previous reports remains limited by HRCT resolution constraints in distinguishing between thin overlying SSCC bone (non-SCD) and true dehiscence (SCD). Three-dimensional volume reconstruction provides a novel method for comprehensive analysis of SCD temporal bone anatomy. We therefore provide an exploratory pilot study to characterize the temporal bone anatomic differences in patients with and without SCD.

2. Methods

This is a retrospective study approved by the Duke University Health System Institutional Review Board. Records were reviewed for 18 adult subjects from 2010 through 2015 presenting to the otology clinic with complaints of vertigo but normal caloric responses, 7 of these subjects (age: 37–67 years, median age is 57 years; gender: 2 males and 5 females) had SCD (per HCRT, audiometry, cervical vestibular evoked myogenic potentials [cVEMP], and clinical findings) and the other 11 subjects (age: 18–84 years, median age is 50 years; gender: 6 males and 5 females) had normal temporal bone anatomy. Of the 7 subjects with SCD 4 subjects had unilateral SCD and 3 subjects had bilateral cases of SCD, thus a total of 10 SCD temporal bones were identified. The methods used for vestibular testing are described elsewhere (Patki et al., 2016). No subjects had surgical or traumatic changes to the temporal bones.

Data collection – Temporal bone CT scans were obtained using a Siemens SOMATOM Definition Flash machine; with a section thickness of 0.6 mm, 512 × 512 matrix, rotation time of 1 s, and exposure time of 1825 ms. Digital imaging and communications in medicine (DICOM) images had 512 rows, 631 columns, and a pixel spacing of 0.176 by 0.176 mm. The scans were imported into and de-identified by Avizo 8.1 software (FEI Visualization Sciences Group, Burlington, MA). Computed anatomic parameters included surface area (SA) in mm^2, volume (V) in mm^3, and surface area-to-volume ratios (SA:V) in mm^{-1} for the following anatomic regions: temporal bone, temporal bone airspaces, and lateral semicircular canals (LSCCs). Temporal bone airspaces were defined as all continuous airspaces medial to the tympanic membrane (TM). The location of the TM was identified at the most lateral sagittal cut showing complete bony encasement of the auditory canal (Fig. 1). For anatomic regions were SA and V were computed, SA was defined as the area of all the surfaces covering that region; V is defined as the amount of space the anatomic region occupies. SA and V were calculated for each anatomic region using Avizo 8.1. To ensure consistency across all scans, the same co-author (M.A.dJ) manually performed all segmentations in the SCD cohort. The distance between the LSCC and TM was measured using ICEM-CFD™ 16.1 software (ANSYS, Canonsburg, PA). Fig. 1 shows the reconstruction of a temporal bone from a CT-scan showing unilateral dehiscence of the right SSCC.

Statistical analysis – Box-plots of computed anatomic parameters (SA, V and SA:V) for temporal bones with SCD from the 7 subjects were compared with normal temporal bones from the 11 subjects, and a two-tailed non-parametric Wilcoxon rank sum test analysis was used to investigate statistical significance at $\alpha = 0.05$. Monothermal warm caloric responses (MV_{warm}) were compared across the 22 unilateral ears from our cohort with normal temporal bones, 10 unilateral ears *affected* by dehisce from the SCD cohort, and 4 unilateral ears *not affected* by dehisce from the SCD cohort. Furthermore, MV_{warm} responses from the 10 unilateral temporal bones *affected* by SCD were plotted against their respective computed temporal bone anatomic parameters (SA, V and SA:V) and linear regression lines were fitted to determine associations between MV_{warm} and dehisced anatomic parameters.

3. Results

As indicated in Fig. 2, temporal bone volume (V) was significantly different between both cohorts ($p = 0.001$). Mean (±standard deviation) temporal bone V in temporal bones with SCD was 16,343 mm^3 ± 4471 mm^3 compared to

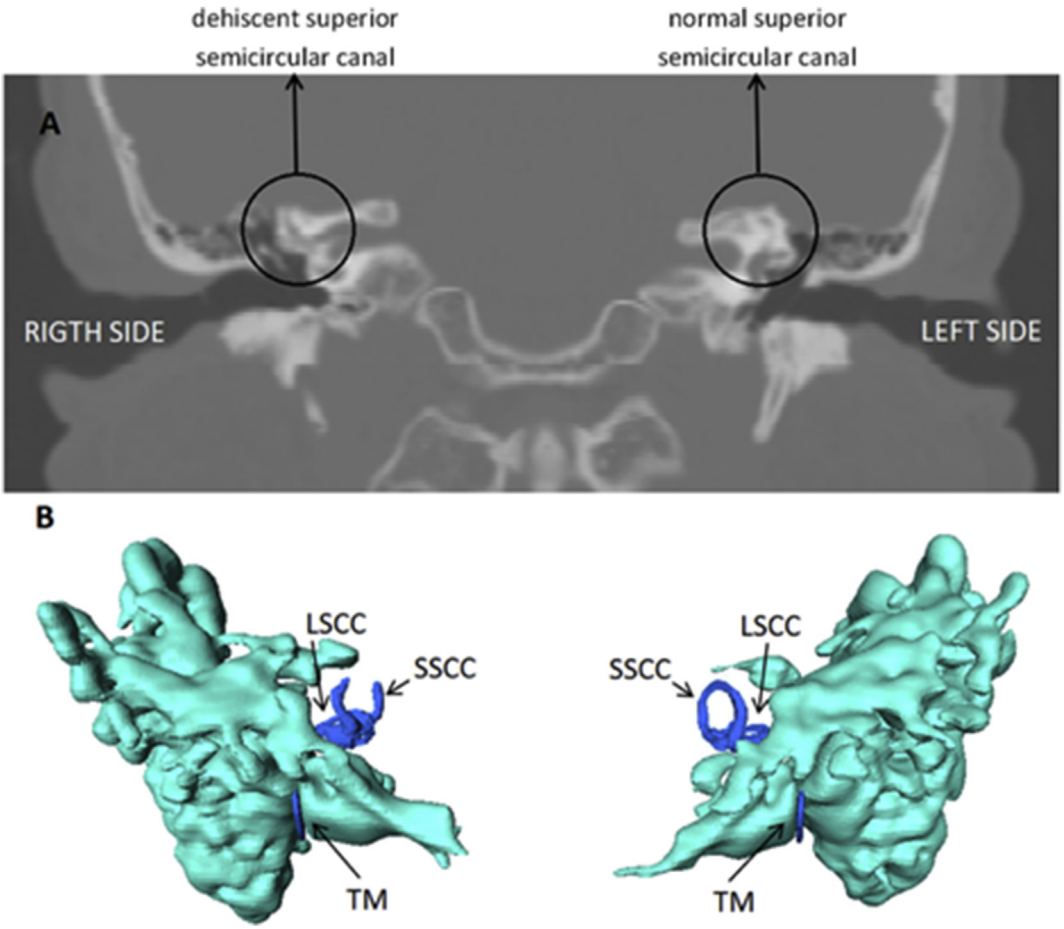

Fig. 1. Temporal bone anatomy in a case of right sided superior semicircular canal dehiscence. A) High resolution CT scan of the temporal bone and B) its 3D reconstruction of the airspace showing unilateral dehiscence of the right superior semicircular canal, while the left superior semicircular canal is covered by bone. The three-dimensional volume reconstruction denotes the temporal bones in light blue and the tympanic membrane and semicircular canals in dark blue. SSCC = superior semicircular canal, LSCC = lateral semicircular canal, TM = tympanic membrane.

21,484 mm^3 ± 3920 mm^3 in those with normal anatomy. Similarly, differences in temporal bone surface area (SA) and SA:V ratio between both cohorts were statistically significant with $p < 0.001$. Average temporal bone SA was higher in the presence of SCD (18,073 mm^2 ± 3002 mm^2) than in temporal bones with normal anatomy (13,733 mm^2 ± 1603 mm^2).

For temporal bone airspace, V, SA, and SA:V were not significantly different between both cohorts; $p = 1$, $p = 0.5$

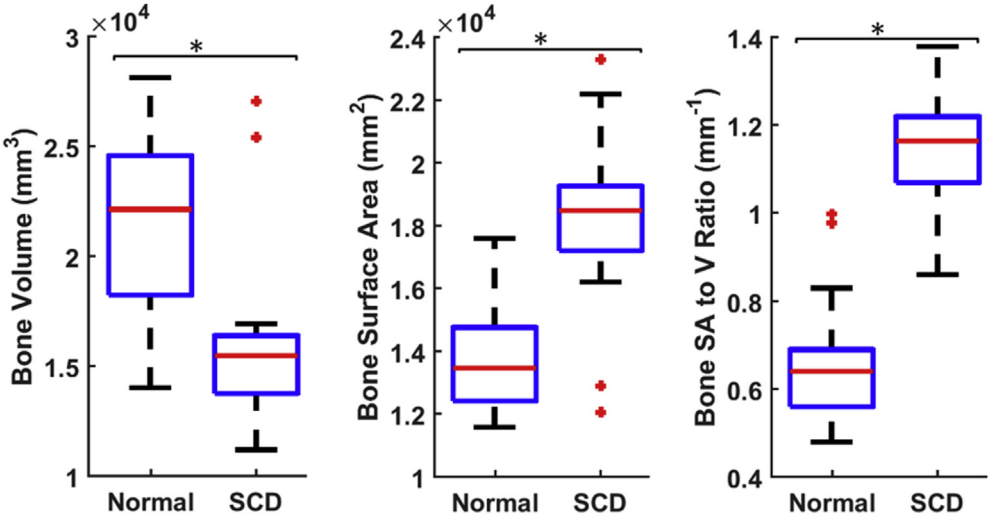

Fig. 2. Box plots with mean values and standard deviation for temporal bone anatomic parameters. Volume, surface area and surface area-to-volume ratio (SA:V) of temporal bones with (n = 10; SCD) and without (n = 22; Normal) superior semicircular canal dehiscence. *Indicates statistical significance at a = 0.05.

and p = 0.2 for analyses on V, SA, and SA:V, respectively. Box-plots figures in Fig. 3 comparing the distributions of both cohorts support the lack of significant differences. With the exception of LSCC SA:V that was significantly different (p = 0.01) between SCD and normal anatomy subjects, computed LSCC values for V (p = 0.2), SA (p = 0.3) and LSCC to TM Distance (p = 0.2) were not significantly different, and these are supported by box-plots in Fig. 4. On average, LSCC V for temporal bones with SCD was higher (12.6 mm^3 ± 2.2 mm^3 vs 11.8 mm^3 ± 5.0 mm^3) with lower SA (59.8 mm^2 ± 8.0 mm^2 vs 64.2 mm^2 ± 11.0 mm^2) than among those with normal temporal bone anatomy. In addition, both LSCC SA:V (4.8 mm^{-1} ± 0.7 mm^{-1}) and LSCC to TM Distance (9.7 mm ± 1.2 mm) for SCD temporal bones were lower than those computed for temporal bones with normal temporal bone anatomy (SA:V = 5.9 mm^{-1} ± 1.5 mm^{-1} and LSCC-to-TM = 9.9 mm ± 0.7 mm).

Average warm caloric response (MV_{warm}) was higher (20.3 ± 10.6 deg/s) in the unilateral ears *not affected* by dehiscence among subjects with SCD than in their unilateral ears *affected* by dehiscence (18.8 ± 9.0 deg/sec). Interestingly, average MV_{warm} was lowest in the unilateral ears from our cohort with normal temporal bones (16.6 ± 8.2 deg/s) compared to temporal bones with SCD (Fig. 5). Plots of MV_{warm} response against computed SCD temporal bone anatomic parameters (SA, V and SA:V) showed moderate to strong correlations between MV_{warm} response and the following anatomic parameters: temporal bone SA:V (r = 0.64), temporal bone airspace V (r = 0.60), temporal bone airspace SA (r = 0.55), LSCC SA (r = 0.51), and LSCC-to-TM Distance (r = 0.65) (see Fig. 6).

4. Discussion

SCD presents a series of clinical and diagnostic challenges. Only recently have improved imaging techniques allowed for the diagnosis of SCD in patients with vertigo (Smullen et al., 1999) and conductive hearing loss (Minor et al., 2003) SCD etiology remains debated. Notably, the thinness of the overlying bone of the SCD has limited the diagnostic utility of HRCT, which has a positive predictive value for SCD of only 57% (Cloutier et al., 2008; Gracia-Tello et al., 2013). The present study characterizes gross anatomic differences between temporal bones with and without SCD. Quantifying these anatomic parameters may assist clinicians where SCD diagnosis is indeterminate based on clinical suspicion and conventional HRCT findings alone.

Our observation that SCD temporal bone volumes are significantly smaller and less dense than normal temporal bone builds upon previous characterization of temporal bone anatomy. Decreased temporal bone pneumatization (i.e. temporal bone airspace) has been demonstrated bilaterally in unilateral SCD patients in comparison to subjects with otosclerosis or temporal bone fracture (Shim et al., 2012). Comparatively, temporal bone thickness has been shown to remain constant bilaterally within normal subjects (Hirvonen et al., 2003; Gracia-Tello et al., 2013). In the current study, the observed differences in temporal bone volume, surface area, and surface area to volume ratio are likely related to SCD morphology rather than baseline bilateral anatomic variation. Therefore, in clinical settings where HRCT findings of the bone overlying the SSCC are indeterminate, the nature and degree of temporal bone asymmetry may affect the diagnostic likelihood of SCD. The ability to analyze multiple anatomic parameters may enable more accurate modeling of temporal bone morphology in future validation studies of SCD diagnosis using three dimensional volume reconstructions.

Calorimetry is the gold standard for testing complaints of dizziness and vertigo in the clinical setting; however, caloric findings are particularly difficult to interpret in patients with temporal bone pathologies because the exact mechanism of heat transfer in the temporal bone remains unknown (Feldmann et al., 1991a,b). It is known that the superior semicircular canal is not reached by caloric irrigation (Ichijo, 2012); however, variations in temporal bone anatomy have been demonstrated to influence

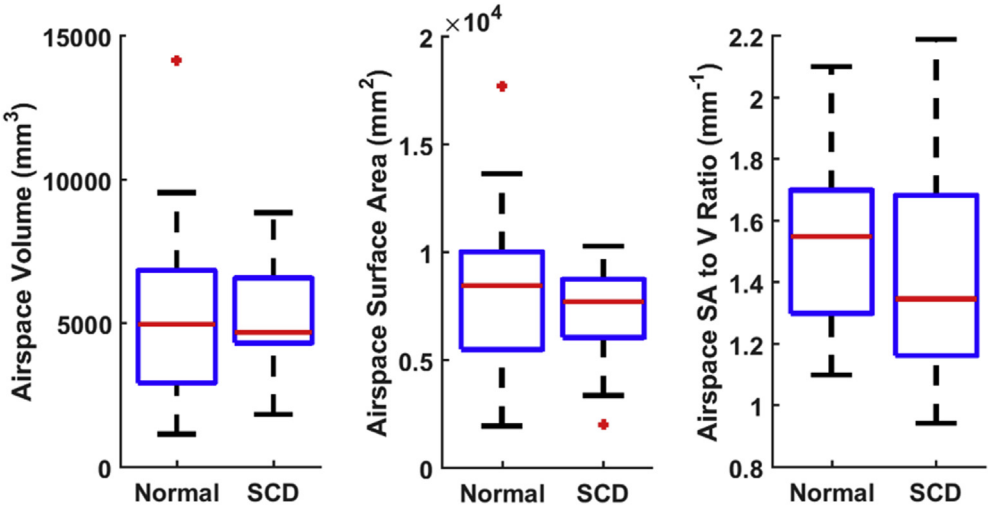

Fig. 3. Box plots with mean values and standard deviation for parameters of temporal bone airspace. Volume, surface area and surface area-to-volume ratio (SA:V) of airspaces of temporal bones with (n = 10; SCD) and without (n = 22; Normal) superior semicircular canal dehiscence.

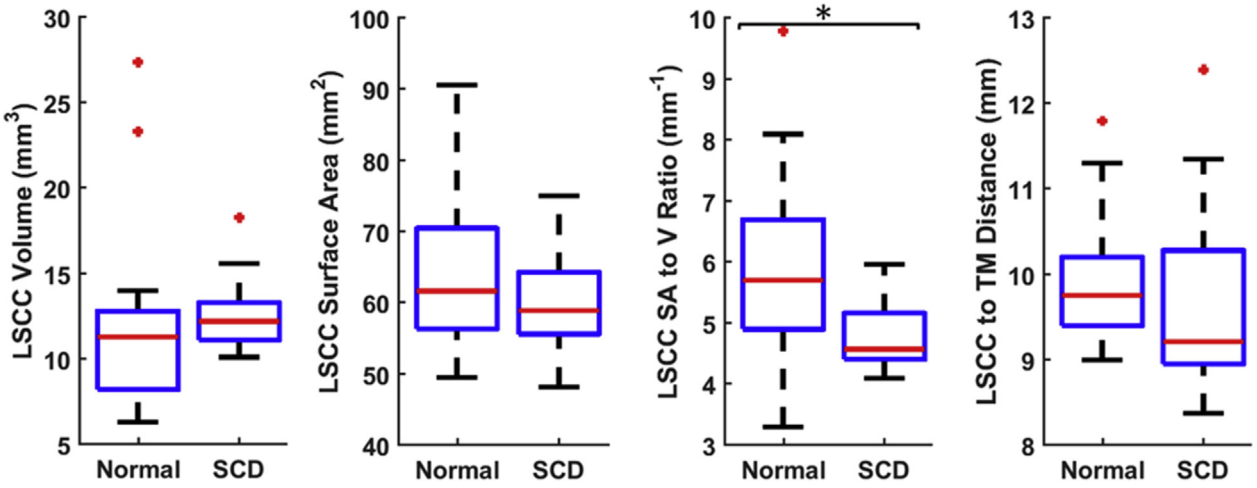

Fig. 4. Box plots with mean values and standard deviation for different extractions of the Lateral Semicircular Canal. Volume, surface area, surface area-to-volume ratio (SA:V) and the distance to the tympanic membrane (TM) of the lateral semicircular canal (LSCC) from temporal bones with (n = 10; SCD) and without (n = 22; Normal) superior semicircular canal dehiscence. *Indicates statistical significance at a = 0.05.

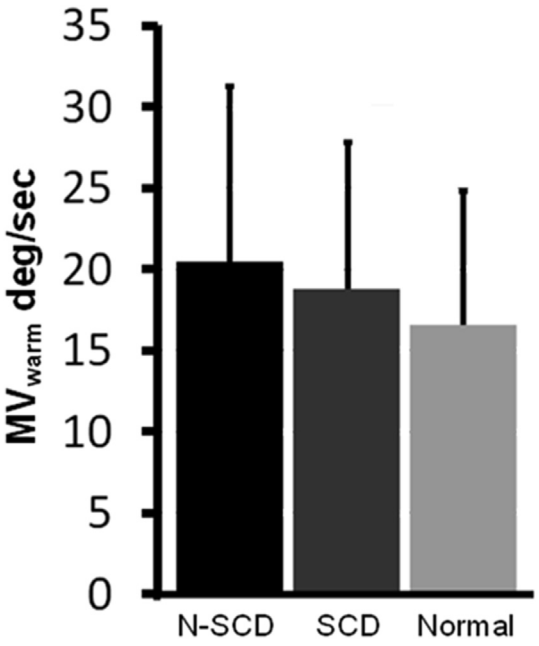

Fig. 5. Caloric response to warm irrigation. Means and standard deviations for the caloric response to warm irrigation (MV_{warm} = maximum velocity of slow phase nystagmus during warm irrigation in degrees/second) are provided for temporal bones with normal anatomy (Normal, n = 22), with SCD (SCD, n = 10), and with normal anatomy from subjects with unilateral superior semicircular canal dehiscence (N-SCD, n = 4).

caloric output (Patki et al., 2016). Specifically, heat may be transferred from the EAC either through bone and soft tissue or by the circulation of air through the middle ear cavity, as observed across a wide variety in anatomic factors of the temporal bone such as total volume and pneumatization (Swarts et al., 2010, 2011; Csakanyi et al., 2011; Cros et al., 2016). Several studies characterizing anatomical differences in temporal bones related to caloric results have reached conflicting conclusions (Harrington, 1969; Zangemeister and Bock, 1979; Proctor, 1982; O'Neill, 1987; O'Neill et al., 1987; Feldmann et al., 1991a,b; Kondoh et al., 2009). However, a recent report, using a novel three-dimensional volume reconstruction technique, showed that a total of 69.5% of the variance in MV_{warm} could be explained by variation in these anatomic factors (Patki et al., 2016). In healthy patients, temporal bone anatomy has been further demonstrated to influence caloric output through a combination of several parameters, rather than significantly through a single variable. The observed univariate correlations between SCD temporal bone anatomy and caloric output appear promising, although a multivariate approach similar to those of reports of healthy subjects is likely necessary. Given our limited sample size and exploratory hypothesis generating approach, modeling the relationship of multiple temporal bone anatomic parameters to caloric output should be further explored in future studies with increased sample sizes.

5. Study limitations

Small sample sizes were due to both low disease prevalence and the amount of labor required per three-dimensional volume reconstruction analysis. Future studies may collect data from multiple institutions, while automating temporal bone volume extraction following three dimensional volume reconstructions is possible. False positives and negative findings on HRCT may have affected our findings, particularly for the four observed cases of unilateral SCD. This possibility emphasizes the need for increased diagnostic accuracy of suspected SCD. A far more sensitive measure in SCD patients is the vestibular evoked myogenic potential (VEMP). Cervical vestibular evoked myogenic potentials (cVEMP) show a reduced threshold and ocular VEMP (oVEMP) peak-to-peak amplitudes are usually increased (Janky et al., 2013; Zuniga et al., 2013). The relationship between VEMP and temporal bone anatomy has never been described in patients with or without SCD, and should be considered in future studies of patients with SCD.

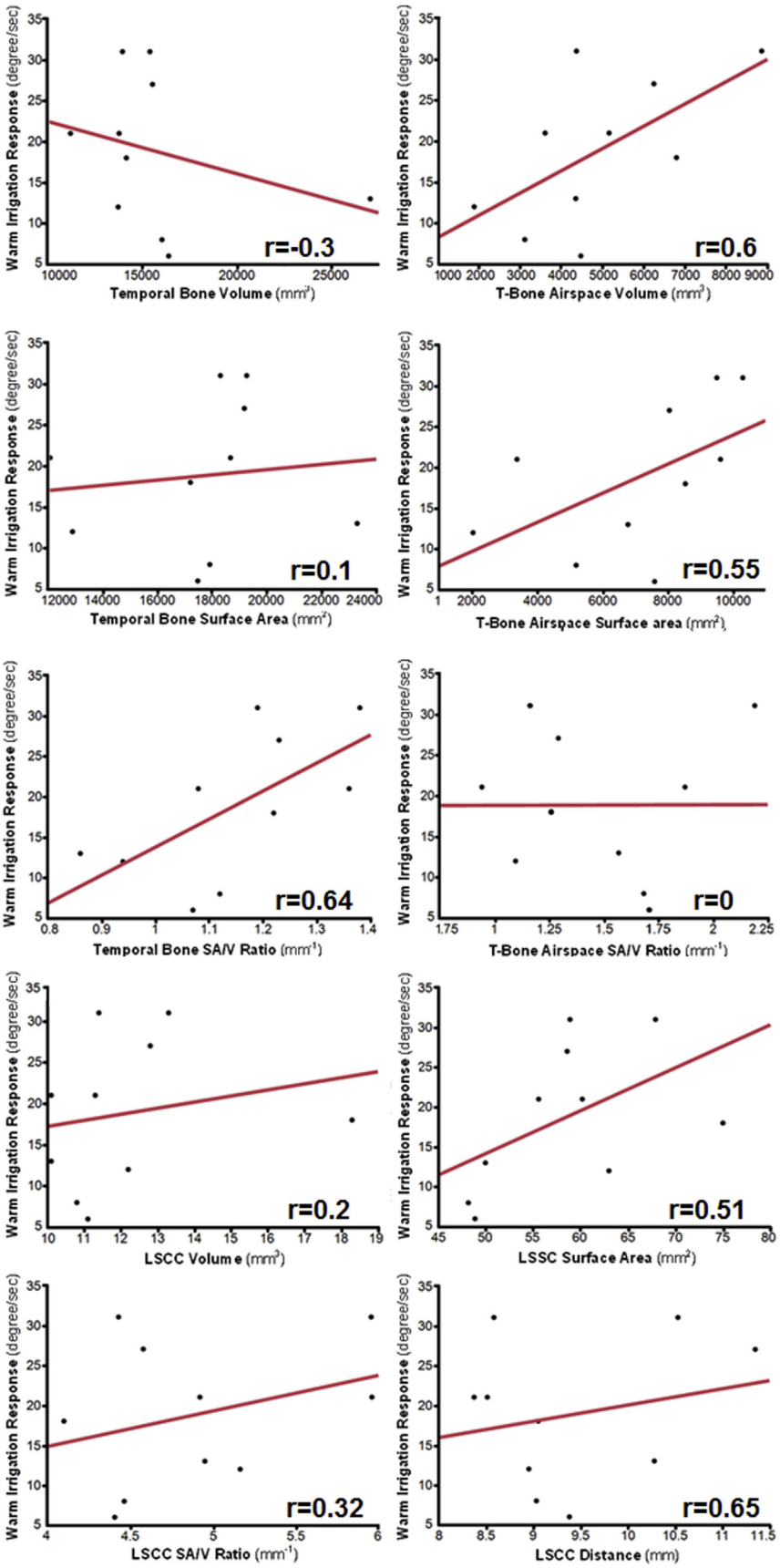

Fig. 6. Correlation of bone and airspace segmentations with caloric responses to warm irrigation. MV_{warm} responses are observed with respect to temporal bone, temporal bone airspace, and lateral semicircular canals for the following parameters: volume, surface area, and surface area/volume ratio for temporal bones with SCD (n = 10).

6. Summary

Gross temporal bone volume is significantly decreased in patients with SCD than in those without SCD. These exploratory data are hypothesis generating as an alternative approach to improving the diagnostic utility of HRCT for SCD.

Financial disclosure and conflict of interest

Dr. de Jong, Carpenter, Kaylie and Frank-Ito report no financial interests or potential conflicts of interest.

Acknowledgments

Research reported in this article was supported in part by the National Institutes of Health (United States of America) under Award Numbers 5T32DC013018-03 and TL1TR001116. The content is solely the responsibility of the authors and does not necessarily represent the official views of the National Institutes of Health. In addition, the authors thank ANSYS, Drs. Paolo Maccarini and Murali Kadiramangalam (ANSYS Global Academic Program Director) for support.

References

Carey, J.P., Minor, L.B., Nager, G.T., 2000. Dehiscence or thinning of bone overlying the superior semicircular canal in a temporal bone survey. Arch. Otolaryngol. Head Neck Surg. 126 (2), 137–147.

Cloutier, J.-F., Bélair, M., Saliba, I., 2008. Superior semicircular canal dehiscence: positive predictive value of high-resolution CT scanning. Eur. Arch. Otorhinolaryngol. 265 (12), 1455–1460.

Cros, O., Knutsson, H., Andersson, M., Pawels, E., Borga, M., Gaihede, M., 2016. Determination of the mastoid surface area and volume based on micro-CT scanning of human temporal bones. Geometrical parameters depend on scanning resolutions. Hear. Res. 340, 127–134.

Csakanyi, Z., Katona, G., Josvai, E., Mohos, F., Sziklai, I., 2011. Volume and surface of the mastoid cell system in otitis media with effusion in children: a case-control study by three-dimensional reconstruction of computed tomographic images. Otol Neurotol. 32 (1), 64–70.

Feldmann, H., Huttenbrink, K.B., Delank, K.W., 1991. Transport of heat in caloric vestibular stimulation. Conduction, convection or radiation? Acta Otolaryngol. 111 (2), 169–175.

Feldmann, H., Hüttenbrink, K., Delank, K., 1991. Transport of heat in caloric vestibular stimulation. Conduction, convection or radiation? Acta Otolaryngol. 111 (2), 169–175.

Gracia-Tello, B., Cisneros, A., Crovetto, R., et al., 2013. Effect of semicircular canal dehiscence on contralateral canal bone thickness. Acta Otorrinolaringol. (English Edition). 64 (2), 97–101.

Harrington, J.W., 1969. Caloric stimulation of the labyrinth experimental observations. Laryngoscope 79 (5), 777–793.

Hirvonen, T.P., Weg, N., Zinreich, S.J., Minor, L.B., 2003. High-resolution CT findings suggest a developmental abnormality underlying superior canal dehiscence syndrome. Acta Otolaryngol. 123 (4), 477–481.

Ho, M.-L., Moonis, G., Halpin, C., Curtin, H., 2017. Spectrum of third window abnormalities: semicircular canal dehiscence and beyond. Am. J. Neuroradiol. 38 (1), 2–9.

Ichijo, H., 2012. Does the superior semicircular canal receive caloric stimulation? Am. J. Otolaryngol. 33 (6), 718–722.

Janky, K.L., Nguyen, K.D., Welgampola, M., Zuniga, M.G., Carey, J.P., 2013. Air-conducted oVEMPs provide the best separation between intact and superior canal dehiscent labyrinths. Otol. Neurotol. 34 (1), 127.

Kondoh, K., Kitahara, T., Morihana, T., Yamamoto, K., Kubo, T., Okumura, S., 2009. Changes in caloric responses after temporal bone surgery with posterior tympanotomy. Auris Nasus Larynx 36 (5), 521–524.

Minor, L.B., Carey, J.P., Cremer, P.D., Lustig, L.R., Streubel, S.-O., 2003. Dehiscence of bone overlying the superior canal as a cause of apparent conductive hearing loss. Otol. Neurotol. 24 (2), 270–278.

O'Neill, G., 1987. The caloric stimulus. Temperature generation within the temporal bone. Acta Otolaryngol. 103 (3–4), 266–272.

O'Neill, G., Calhoun, E., Francis, K., Chui, P., Hayward, C., 1987. The influence of temporal bone anatomical variation upon the caloric stimulus. Clin. Otolaryngol. Allied Sci. 12 (4), 277–282.

Patki, A.U., Ronen, O., Kaylie, D.M., Frank-Ito, D.O., Piker, E.G., 2016. Anatomic variations in temporal bones affect the intensity of nystagmus during warm caloric irrigation. Otol. Neurotol. 37 (8), 1111–1116.

Proctor, L.R., 1982. The effect of variations in temporal bone structure upon the caloric response. Acta Otolaryngol. 94 (3–4), 253–259.

Shim, B.S., Kang, B.C., Kim, C.-H., Kim, T.S., Park, H.J., 2012. Superior canal dehiscence patients have smaller mastoid volume than age-and sex-matched otosclerosis and temporal bone fracture patients. Korean J. Audiol. 16 (3), 120–123.

Smullen, J., Andrist, E., Gianoli, G., 1999. Superior semicircular canal dehiscence: a new cause of vertigo. J. La. State Med. Soc. 151 (8), 397–400.

Swarts, J.D., Cullen Doyle, B.M., Alper, C.M., Doyle, W.J., 2010. Surface area-volume relationships for the mastoid air cell system and tympanum in adult humans: implications for mastoid function. Acta Otolaryngol. 130 (11), 1230–1236.

Swarts, J.D., Doyle, B.C., Doyle, W.J., 2011. Relationship between surface area and volume of the mastoid air cell system in adult humans. J. Laryngol Otol. 125 (06), 580–584.

Zangemeister, W., Bock, O., 1979. The influence of pneumatization of mastoid bone on caloric nystagmus response: a clinical study and a mathematical model. Acta Otolaryngol. 88 (1–6), 105–109.

Zuniga, M.G., Janky, K.L., Nguyen, K.D., Welgampola, M.S., Carey, J.P., 2013. Ocular vs. cervical VEMPs in the diagnosis of superior semicircular canal dehiscence syndrome. Otol. Neurotol 34 (1), 121.